Supporting Online Material for

Experience-Driven Plasticity of Visual Cortex Limited by Myelin and Nogo Receptor

Aaron W. McGee, Yupeng Yang, Quentin S. Fischer,
Nigel W. Daw, Stephen M. Strittmatter*

To whom correspondence should be addressed. E-mail: stephen.strittmatter@yale.edu

Published 30 September 2005, *Science* **309**, 2222 (2005)
DOI: 10.1126/science.1114362

This PDF file includes:

Supplemental On-Line Material

Methods

Mouse genetic models

The Nogo-A/B gene trap and NgR gene targeted mouse strains have been described (*1*, *2*). All experiments were performed on a mixed C57Bl6 and 129 mouse strain background. The targeted ES cells were derived from the 129 strain and were implanted into a C57Bl6 blastocyst. Chimeras were backcrossed to C57Bl6 mice for 4-7 generations prior to the experiments here which utilized littermate controls in all cases.

Immunohistochemistry and Immunoblotting

Mice were deeply anesthetized with intramuscular ketamine (100 mg/kg) and intraperitoneal xylazine (15 mg/kg) and perfused transcardially with PBS followed by 4% PFA in PBS. Brains were removed post-fixed for one hour. Fifty μm thick free-floating coronal sections were cut at room temperature with a vibratome. Sections were stained using standard procedures with antibodies against parvalbumin (Chemicon, 1:500), myelin basic protein (MBP) (Sternberger monoclonals, 1:500), NgR (1:500), GAD65 (R&D Systems, 10 μg/ml), Parvalbumin (Chemicon, 2 μg/ml) or with the lectin WFA (Vector labs, 5μg/ml) as indicated, followed by the appropriate Alexa488/568 secondary antibodies or for WFA, a Cy3-conjugated streptavidin (Sigma). Sections were stained with Hoescht 33342 (2μg/ml) to identify cell nuclei. Images were collected at 10X with an Olympus FV12 camera and merged with the software Photoshop (Adobe). For confocal microscopy, images were obtained from fifty-micron thick coronal sections using a 60X water immersion objective (NA 1.2) mounted on a Nikon TE2000-U

inverted microscope. Samples were scanned with a Bioradiance 2100MP laser controlled by Lasersharp acquisition software. Laser intensity, iris diameter, gain and offset settings were identical for all images collected. Images are the averages of three monoplanar scans (Kalman). Mean pixel intensity for GAD65 staining in the neuropil and the density of parvalbumin-positive neurons was performed as described by Huang et. al. (*3*) .

For immunoblotting, the binocular zone of primary visual cortex (L2-4 mm, P0-2mm) from two animals for each sample at each age was dissected away from the underlying white matter with a micro dissecting knife with the aid of a Zeiss Stemi DV4 dissecting scope under trans-illumination. The tissue was homogenized in RIPA buffer (1% Triton/0.5% sodium deoxycholate/0.1%SDS/PBS/2mm DTT). After sonication and centrifugation, supernatants were collected and protein concentrations determined with the Amersham 2D Quant kit. Multiple standards and sample duplicates were measured concomitantly to insure accuracy. 20 μg of protein was separated by SDS-PAGE and Western blotting was performed with anti-MBP, Nogo, NgR, MAG, GAD65 (0.2 μg/ml) and tPA (US Biological, 1:1000) antibodies as previously described(*2*). The specificity of the anti-tPA antibody has been demonstrated in studies of tissue from tPA -/- mouse brain (*4*).

The relative abundance of GAD65 and tPA in protein extracts from visual cortex prepared as described (above) for four samples for both genotypes Blots were developed with alkaline-phosphatase-coupled secondary antibodies (Sigma) using a chromogenic substrate. Samples were quantified as the mean density of a small rectangle enclosing the band with the ‘measure’ function of NIH Image version 1.63. Measurements were taken from at least three independent samples run in duplicate on the same gel for both P60 WT

and NgR KO mice. The mean density measurements for WT and NgR KO were normalized against the average for the WT samples and expressed as a percentage.

Analysis of MBP distribution

Images from anti-MBP /Alexa488 and Hoescht 33258-stained coronal sections containing visual cortex were captured at 10X and merged in Photoshop. At least two images were required to span the distance from the subcortical white matter to the pial surface. Hoescht staining was utilized to identify visual cortex prior to capturing images of MBP staining. Data points are the average of at least four sections from each of three animals for each age and genotype. Fluorescence intensity at the subcortical white matter was normalized and images were imported into NIH Image J. The relative distribution of fluorescence intensity was measured using the profile function of Image J and the corresponding pixel intensities were reported. All statistical comparisons were performed with Student's two-tailed *t*-test.

Electrophysiology

Electrophysiological recordings were performed under Nembutal (50 mg/kg, i.p.; Abott) /chlorprothixene (10 mg/kg, i.m; Sigma) anesthesia using standard procedures(5). Atropine (20mg/kg, s.c.; Optopic) was injected to reduce secretions and the parasympathetic effects of anesthetic agents, and dexamethasone (4 mg/kg, s.c.; American Reagent) was administered to reduce cerebral edema. The mouse was placed in a stereotaxic device after a tracheal tube and i.p. cannula were inserted. A craniotomy was made over the right visual cortex, and agar was applied to enhance recording

stability and prevent desiccation. The eyelids were removed from both eyes and the corneas protected thereafter by frequent application of silicon oil. Animal temperature was maintained at 37°C by a homeostatically-controlled heating pad. Heart rate and respiration were monitored continuously.

The electophysiological responses for 4-6 cells separated by > 90 μm in depth were recorded for each electrode penetration. In each mouse, 4 to 6 separate penetrations were spaced evenly at least 200 μm apart across the binocular region, defined by a RF azimuth of < 25 degrees. Cells were assigned to OD categories according to the 7-category scheme of Hubel and Wiesel(*6*) based on the auditory discrimination of an investigator blind to the genotype, deprivation history, and age of the animal. OD histograms were constructed and weighted ocular dominance (WOD) scores were calculated for each mouse with the formula: WOD = (1/6G2+2/6G3+3/6G4+4/6G5+5/6G6+G7)/N, where Gi is the number of cells in OD group i, and N is the total number of cells. Most units were also scored for noise and response strengths on a 1 (weak noise/response firing) to 3 (strong noise/response firing) scale. All comparisons were evaluated with Student's two-tailed *t*-test.

Monocular deprivation

Lid suture of the left eye was performed under 1-2% halothane anesthesia. Lid margins were trimmed and the lids sutured together using 6-0 silk. After four days of monocular deprivation the lid was opened and visual responses were recorded from animals as described(*5*).

Dark rearing

Tissue from dark reared mice was generously provided by Dr. Ning Tian (Yale univ., New Haven, CT). Dark rearing methodology has been described (*7-9*).

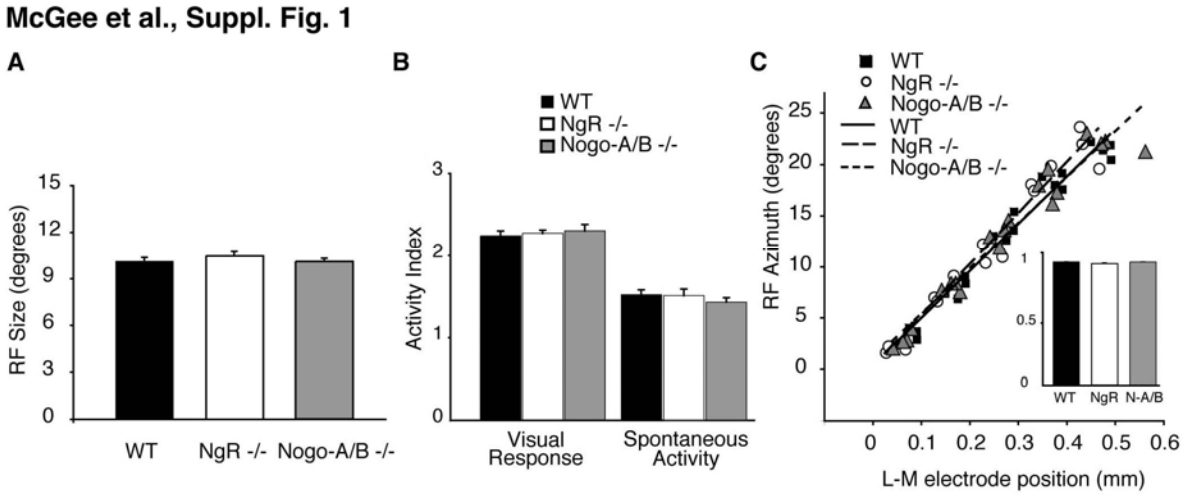

Supplemental Figure 1 Neuronal responses in visual cortex are unchanged in NgR and Nogo-A/B mutant mice. **A**, Receptive field (RF) area in wild-types (C57Bl6) (n = 8), NgR mutants (n= 8) and Nogo-A/B mutants (n = 9) (WT vs. NgR, p = 0.35; WT and N-A/B, p = 0.14). **B**, Stimulus evoked and spontaneous activity (p > 0.28 in all comparisons). **C**, Regressions of RF-center azimuth versus lateromedial electrode position for WT (black squares, n = 4), NgR (open circles, n = 3) and Nogo-A/B (grey triangles, n = 4) mutants. Insets are correlation coefficients (WT = 8, NgR = 8, Nogo-A/B = 9; WT vs. NgR, p = 0.61; WT vs. N-A/B, p = 0.14).

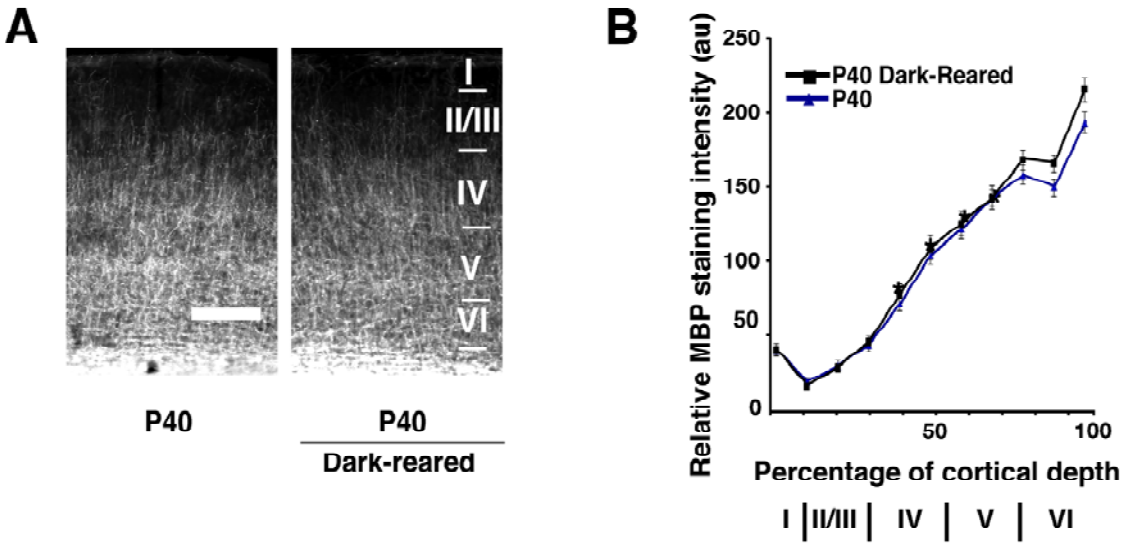

Supplemental Figure 2. Dark rearing does not affect the maturation of intracortical myelination in visual cortex. **A**, P40 visual cortex from normally housed (12 hr light/dark cycle) or dark-reared (24 hr dark) labelled with antibodies to MBP. Layers I-VI are indicated (right). Scale bar = 200 μm. **B**, Distribution of relative MBP intensity within visual cortex for P40 normal or dark-reared animals. Error bars = ±SEM where the variance is the number of animals (n=3).

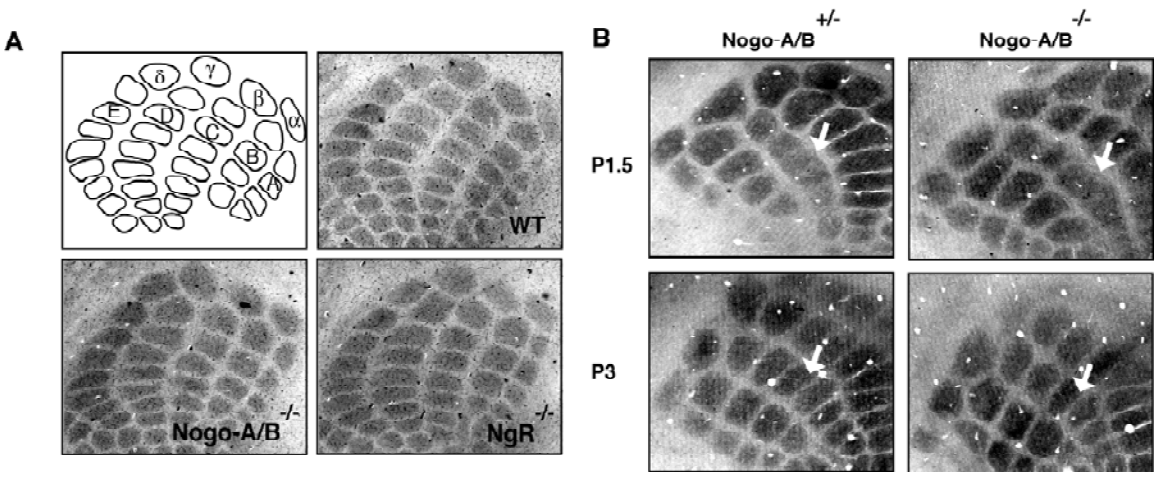

Supplemental Figure 3. Barrel plasticity is unaltered in NgR and Nogo-A/B mutant mice. A, A schematic illustrating the position of barrels corresponding to whisker rows A – E (upper left).The barrel pattern in flattened sections of somatosensory cortex revealed by cytochrome oxidase staining is indistinguishable between WT (upper right), Nogo-A/B (lower left) and NgR (lower right) mutant mice. B, Representative images of barrel cortex of Nogo-A/B mutants and heterozygous littermates following whisker ablation during (P1.5) or after (P3) the critical period. White arrows indicate the compression and fusion of barrels in the C row after whisker ablation at P1.5 but not P3.

References

1. J. E. Kim, B. P. Liu, J. H. Park, S. M. Strittmatter, *Neuron* **44**, 439 (Oct 28, 2004).
2. J. E. Kim, S. Li, T. GrandPre, D. Qiu, S. M. Strittmatter, *Neuron* **38**, 187 (Apr 24, 2003).
3. Z. J. Huang *et al.*, *Cell* **98**, 739 (Sep 17, 1999).
4. F. J. Salles, S. Strickland, *J Neurosci* **22**, 2125 (Mar 15, 2002).
5. Q. S. Fischer *et al.*, *J Neurosci* **24**, 9049 (Oct 13, 2004).
6. T. N. Wiesel, D. H. Hubel, *J Neurophysiol* **26**, 1003 (Nov, 1963).
7. N. Tian, *Vision Res* **44**, 3307 (Dec, 2004).
8. N. Tian, D. R. Copenhagen, *Neuron* **39**, 85 (Jul 3, 2003).
9. N. Tian, D. R. Copenhagen, *Neuron* **32**, 439 (Nov 8, 2001).